Short-imaginary-time quantum critical dynamics in the J-Q_3 spin chain

Yu-Rong Shu [1,2] and Shuai Yin [3,*]

[1] *School of Physics and Materials Science, Guangzhou University, Guangzhou 510006, China*

[2] *Research Center for Advanced Information Materials, Guangzhou University, Guangzhou 510006, China*

[3] *School of Physics, Sun Yat-Sen University, Guangzhou 510275, China*

(Received 26 June 2020; revised 3 September 2020; accepted 4 September 2020; published 21 September 2020)

We study the short-imaginary-time quantum critical dynamics (SITQCD) in the J-Q_3 spin chain, which hosts a quasi-long-range-order phase to a valence bond solid transition. By using the scaling form of the SITQCD with a saturated ordered phase, we are able to locate the critical point at $q_c = 0.170(14)$. We also obtain the critical initial slip exponent $\theta = -0.507(3)$ and the static exponent $\beta/\nu = 0.498(2)$. More strikingly, we find that the scaling dimension of the initial order parameter x_0 is close to zero, which suggests that the initial order parameter is a marginal operator. As a result, there is no initial increase behavior of the order parameter in the short-imaginary-time relaxation process for this model, which is very different from the relaxation dynamics in the Ising-type phase transitions. Our numerical results are realized by the projector quantum Monte Carlo algorithm.

DOI: 10.1103/PhysRevB.102.104425

I. INTRODUCTION

Nonequilibrium dynamics of quantum phase transitions has been an attractive topic in condensed-matter physics and statistical physics in recent decades [1,2]. Among different types of nonequilibrium dynamics, the quantum imaginary-time relaxation stands out as a usual method to find the ground state of quantum many-body systems. Moreover, algorithms based on the imaginary-time relaxation were designed for quantum computations recently [3,4]. In addition, studies on the imaginary-time evolution also reap great benefits [5–9]. For example, it was shown that in the driven critical dynamics, the imaginary- and real-time dynamics have considerable similarities [5], but the former is much easier to realize numerically, especially for systems in higher dimensions [5–7,10]. In addition, by comparing with the classical short-time critical dynamics in dissipative systems [11–13], the scaling theory for the short-imaginary-time quantum critical dynamics (SITQCD) was developed [14,15] by analogy with its classical counterparts [16–20]. This theory provides efficient methods to determine the critical properties in the short-time region, overcoming the difficulties induced by the critical slowing down [14,15,21].

In imaginary-time evolution, the system is controlled by low-lying energy levels so that universal power-law behaviors can exist during the evolution after a transient microscopic time [14,15,22]. In the Ising-type phase transition, the SITQCD theory shows that the critical initial slip of the order parameter $D(\tau) \propto D_0 \tau^{\theta}$ exists when an initial state with small D_0 and zero correlation is prepared. Therein θ is the critical initial slip exponent and is positive for the quantum Ising model in both one and two dimensions [14,15,21]. Namely, with a small initial value D_0, in the early stage of the evolution, $D(\tau)$ does not decrease towards its ground-state value of zero. Instead, $D(\tau)$ counterintuitively experiences an increasing stage, which scales as $\tau_{cr} \sim D_0^{-z/x_0}$, with x_0 being the scaling dimension of D_0 [14,15,21]. For the quantum Ising model in both one and two dimensions, x_0 is positive, and D_0 is a relevant scaling variable, resulting the initial increase of $D(\tau)$.

Here, we study the SITQCD of the one-dimensional J-Q_3 model by means of quantum Monte Carlo (QMC) simulations. The Hamiltonian of the J-Q_3 chain is given by [23,24]

$$H = -J \sum_{i=1}^{L} P_{i,i+1} - Q \sum_{i=1}^{L} P_{i,i+1} P_{i+2,i+3} P_{i+4,i+5}, \qquad (1.1)$$

where J and Q are both antiferromagnetic (AF) couplings and $P_{i,i+1}$ denotes the two-spin singlet operator

$$P_{i,i+1} = \tfrac{1}{4} - \mathbf{S}_i \cdot \mathbf{S}_{i+1}. \qquad (1.2)$$

The standard J interactions tend to form the quasi-long-range-order (QLRO) phase that is in the class of the standard critical Heisenberg chain, while the multispin Q terms favor a doubly degenerate valence bond solid (VBS) phase. A transition appears at $q_c = (Q/J)_c \approx 0.16$ [24,25], separating the QLRO phase from the VBS phase. The same kind of phase transition also occurs in the well-studied J_1-J_2 spin chain [26,27] at the coupling ratio $J_2/J_1 = 0.241167(5)$ [27]. However, due to the "sign problem" caused by the next-nearest-neighbor frustrating J_2 interactions, QMC simulations of the J_1-J_2 model are hardly available. In addition, a related J-Q_2 chain in the same J-Q family also has similar properties, but the VBS order is weaker in it [23,24]. In two dimensions, the J-Q model exhibits a fascinating deconfined quantum phase transition between the Néel and VBS phases [23].

*yinsh6@mail.sysu.edu.cn

The rest of the paper is organized as follows. In Sec. II, we review the SITQCD theory and the scaling relations that are useful in our study. The QMC method employed in this work is outlined in Sec. III. We present our numerical results in Sec. IV and discuss our findings in Sec. V. A summary is given in Sec. VI.

II. SHORT-IMAGINARY-TIME QUANTUM CRITICAL DYNAMICS SCALING THEORY

For a quantum state $|\Psi(\tau)\rangle$, the imaginary-time evolution of the wave function is described by the imaginary-time Schrödinger equation [28,29]. Near the critical point, $|\Psi(\tau)\rangle$ is governed by the low-energy levels during the imaginary-time evolution as the high-energy levels decay very fast. According to the theory of SITQCD, observable $\mathcal{O}$ should obey the following scaling form [14,15]:

$$\mathcal{O}(\tau, g, D_0, L) = b^{\phi}\mathcal{O}(\tau b^{-z}, g b^{\frac{1}{\nu}}, D_0 b^{x_0}, L b^{-1}), \tag{2.1}$$

in which τ, g, D_0, and L represent the imaginary time, the distance to the critical point, the initial value of the order parameter, and the system size, respectively. z is the dynamic exponent, and ν is the correlation length exponent. x_0 is the dimension of D_0, and ϕ is related to the quantity $\mathcal{O}$ studied. For instance, $\phi = -\beta/\nu$ (with β being the order parameter exponent) for the order parameter, and $\phi = 0$ for the dimensionless variable. There are two *apparent* fixed points that can be readily identified for D_0: One is $D_0 = 0$; the other is $D_0 = D_{\rm sat}$, with $D_{\rm sat}$ being the maximum value of D (the saturated value, which depends on the model studied). $D_0 = 0$ and $D_0 = D_{\rm sat}$ represent completely disordered and ordered states, respectively, which do not change under scale transformation. Moreover, these two fixed points do not depend on the scaling dimension of D_0.

By choosing the scaling factor $b = \tau^{\frac{1}{z}}$, one obtains the scaling form of $\mathcal{O}$,

$$\mathcal{O}(\tau, g, D_0, L^{-1}) = \tau^{\frac{\phi}{z}} f_{\mathcal{O}}(g\tau^{\frac{1}{\nu z}}, D_0\tau^{\frac{x_0}{z}}, L^{-1}\tau^{\frac{1}{z}}), \tag{2.2}$$

in which $f_{\mathcal{O}}$ is the scaling function related to $\mathcal{O}$. For small D_0, in the short-time region, $f_{\mathcal{O}}$ can be expanded as a series of $D_0\tau^{\frac{x_0}{z}}$. Note that the correlation length ξ of the initial state has to be very short as required by the SITQCD theory [11,14]. With $\xi \to 0$, the derivatives of the free energy are analytic. In addition, in the short-time region, $f_{\mathcal{O}}$ is a continuous function of $D_0\tau^{\frac{x_0}{z}}$, so that one can perform series expansion of $f_{\mathcal{O}}$ in terms of $D_0\tau^{\frac{x_0}{z}}$. Such treatment has proven to be valid in both classical short-time critical dynamics [11] and the SITQCD theory [14] already. Taking the order parameter D for an example, the leading part of the scaling form obeys

$$D(\tau, g, D_0, L^{-1}) = D_0\tau^{\theta} f_D(g\tau^{\frac{1}{\nu z}}, L^{-1}\tau^{\frac{1}{z}}), \tag{2.3}$$

in which the critical initial slip exponent θ reads

$$\theta = \frac{x_0}{z} - \frac{\beta}{\nu z}. \tag{2.4}$$

When $\theta > 0$, the order parameter increases in the initial stage of the evolution. This is the case for the quantum Ising model in both one and two dimensions [14,21]. Therein the initial order parameter is relevant, and x_0 is larger than β/ν.

However, when the initial order parameter is marginal, i.e., $x_0 = 0$, Eq. (2.4) gives $\theta = -\frac{\beta}{\nu z}$. In this situation, the order parameter will not increase with τ. Instead, it will decay as $D \sim D_0\tau^{-\frac{\beta}{\nu z}}$, similar to its long-time relaxation. We will find that this is just the case for the J-Q_3 spin chain (1.1) studied here.

Moreover, when the initial order parameter D_0 is chosen at its apparent fixed points, i.e., $D_0 = 0$ or $D_0 = D_{\rm sat}$, Eq. (2.1) shows that the kth moment of the order parameter with D_0 being at its fixed point satisfies

$$D^k(\tau, L^{-1}) = \tau^{-k\frac{\beta}{\nu z}} f_{D^k, D_0}(g\tau^{\frac{1}{\nu z}}, L^{-1}\tau^{\frac{1}{z}}). \tag{2.5}$$

Besides the order parameter, the SITQCD behavior also manifests in the imaginary-time correlation function of D [12,21,30],

$$C(\tau) = \lim_{D_0 \to 0} \frac{D(\tau)}{D_0} = L\langle \hat{D}(0)\hat{D}(\tau)\rangle, \tag{2.6}$$

in which $\hat{D}$ is the operator of the dimer order parameter at imaginary time 0 and τ. Here, $\langle\cdots\rangle$ represents the statistical average of the operators. It has been shown that $C(\tau)$ satisfies $C(\tau) \propto \tau^{\theta}$ in the thermodynamic limit, while for finite-size systems, the scaling form of $C(\tau)$ at the critical point is [12,21,30]

$$C(\tau, L) = \tau^{\theta} f_C(\tau L^{-z}). \tag{2.7}$$

According to Eq. (2.7), when the initial order parameter is marginal, $C(\tau)$ decays as $C(\tau) \sim \tau^{-\frac{\beta}{\nu z}}$, as will be seen in the J-Q_3 chain.

The scaling theory of the SITQCD can be employed to determine the critical properties [14,15,21]. For example, to determine the critical point, the initial order parameter D_0 can be chosen to be its fixed values to lessen the variables in Eq. (2.2). In this situation, the dimensionless variable, such as the average sign of the order parameter $I(\tau)$, defined as $I(\tau) = \langle \mathrm{sgn}\{D(\tau)\}\rangle$ [31,32], satisfies

$$I(\tau, g) = f_I(\tau L^{-z}, L^{\frac{1}{\nu}} g). \tag{2.8}$$

For a fixed aspect ratio τL^{-z}, Eq. (2.8) shows that $I(\tau, g)$ cross at $g = 0$ for different system sizes. Accordingly, the critical point can be determined. In addition, by using Eq. (2.5) at $g = 0$, one can determine the static exponent β/ν. Moreover, θ can be estimated from Eqs. (2.3) and (2.7). For the case where D_0 is relevant, Eq. (2.7) is simpler in practice as it takes the limit $D_0 \to 0$ in advance.

III. NUMERICAL METHOD

In this section, we will introduce the QMC method used in our calculations briefly. The projector QMC method employed in this work is based on the stochastic series expansion (SSE) QMC method [10].

In imaginary time, the Schrödinger equation describes the evolution of a quantum state $|\Psi(\tau)\rangle$ as [28,29]

$$\partial_\tau |\Psi(\tau)\rangle = -H|\Psi(\tau)\rangle. \tag{3.1}$$

A formal solution of the Schrödinger equation is given by

$$|\Psi(\tau)\rangle = U(\tau)|\Psi(\tau_0)\rangle, \tag{3.2}$$

in which $U(\tau) = e^{-\tau H}$ is the imaginary-time evolution operator and τ_0 is the starting time of the evolution. The expectation value of an operator $\hat{\mathcal{O}}$ at τ is then

$$\mathcal{O}(\tau) = \frac{1}{Z}\langle\Psi(\tau)|\hat{\mathcal{O}}|\Psi(\tau)\rangle, \tag{3.3}$$

where the normalization is defined as

$$Z = \langle\Psi(\tau)|\Psi(\tau)\rangle = \langle\Psi(\tau_0)|e^{-\tau H}e^{-\tau H}|\Psi(\tau_0)\rangle. \tag{3.4}$$

The central idea of the projector QMC method is to perform series expansion of $U(\tau)$ in the normalization

$$Z = \sum_n^{\infty}\sum_{S_n}\langle\Psi(\tau_0)|\frac{\beta^n}{n!}S_n|\Psi(\tau_0)\rangle, \tag{3.5}$$

with S_n denoting the operator sequence and $\beta = 2\tau$. The expansion order n can be truncated to some maximum length that causes no detectable error. The operator sequence and states are then importance sampled, and measurements can be done accordingly. To gain efficiency, we employ a global loop-update scheme in the importance sampling procedure [10,33]. In our calculations, we perform 10^5 equilibration steps followed by at least 100 bins of successive measurements, each with 10^5 Monte Carlo steps, in order to ensure statistical errors are under control.

In comparison with the SSE method, in the projector method, the imaginary-time axis can have different or fixed boundary states, which is actually crucial for realizations of different initial states in this study. In addition, for short evolution times, a binomial weight factor should also be inserted in Eq. (3.5) in order to obtain accurate expectation values as different propagated states have different contributions when τ is not large. At long times, the effect of the weight factor becomes negligible, and the measurements can be done in the "middle" of the projection axis far away from the boundaries [33].

In addition, in the projector QMC method, apart from the standard S^z basis, the valence bond basis can also be applied [24,34]. Here, we consider different initial states, including VBS, AF, and disordered states. The valence bond basis has $S^z_{\rm tot} = 0$ so that it is convenient in realizing VBS states. For disordered and AF states, the standard S^z basis is more useful. Therefore, in our calculations, different bases will be used according to the initial state. Both the SSE and projector QMC methods are well documented, and here, we refer readers to details of the methods in the literature [10,33,34].

IV. NUMERICAL RESULTS

In this section, we present the QMC results of the SITQCD in the QLRO-VBS transition of the J-Q_3 chain. First, we locate the critical point of the transition and then compute the critical initial slip exponent θ. The static exponent ratio β/ν is then determined. By comparing θ and β/ν, we find that their absolute values are almost equal to each other, namely, x_0 very close to zero, indicating a marginal D_0. The dynamical exponent z of the J-Q_3 chain is known to be $z = 1$ [10], which will be set as the input.

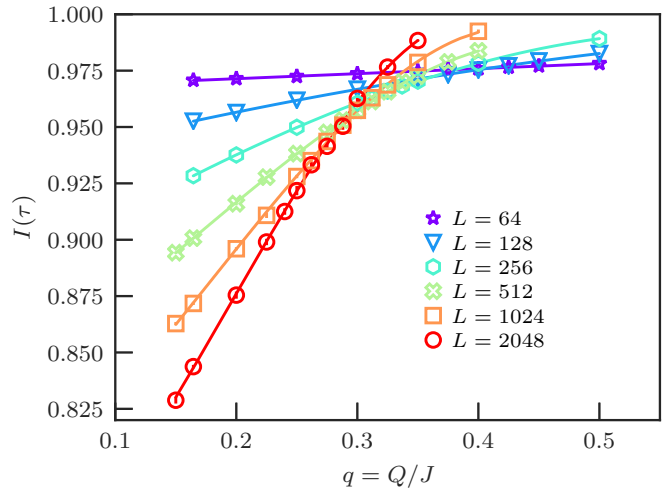

FIG. 1. $I(\tau)$ for different coupling ratios $q = Q/J$ with sizes from $L = 64$ to 2048 at $\tau L^{-z} = 1/16$. The error bars are much smaller than the symbols (which is also the case in other figures). The solid lines are polynomial fits to the data, up to cubic terms.

In the J-Q_3 chain, the order parameter for the dimer order is defined as $D = [\sum_i^L (-1)^i \mathbf{S}_i \cdot \mathbf{S}_{i+1}]/L$ or its z component D_z. In the following, for simplicity, the full dimer order parameter and its z component are both denoted as D.

A. Determination of the critical point

To locate the critical point, the system is prepared in the VBS initial state and then relaxes in the imaginary time. Here, $D_{\rm sat} = 3/8$ (full order parameter). We compute $I(\tau)$ for $L = 48$ to 2560 with a fixed aspect ratio $\tau L^{-z} = 1/16$. In Fig. 1, we plot $I(\tau)$ for $L = 64$ to 2048 to show how the crossing point of L and $2L$ evolves with the increase of L. The values of $I(\tau)$ are close to 1 for all coupling ratios q, indicating that the system remains mostly in the VBS phase. It is obvious that the evolution time $\tau = L^z/16$ is too short for the system to get rid of the remanence of the initial VBS state.

Using polynomials up to cubic terms to fit the data, we can extract the crossing point q_c of $I(\tau)$ for L and $2L$. The dependence of q_c on the system size L is shown in Fig. 2. Unlike the usual cases where $q_c(L)$ converges rapidly as L increases, here, $q_c(L)$ exhibits a convex behavior, which suggests that the size effect in q_c is not negligible even at the largest-size system accessed. We use the form $q_c(L) = q_c + aL^{-\omega}$ [35] to fit $q_c(L)$ and find that in the limit of $L \to \infty$, q_c is 0.170(14), which agrees with the exact diagonalization (ED) result $q_c = 0.16478(5)$ given in a recent study [36].

In the inset of Fig. 2, we show the dependence of q_c on the fitting range by changing the largest system size $L_{\rm max}$ included in the fitting. As $L_{\rm max}$ increases, q_c approaches the ED result $q_c = 0.16478(5)$ rapidly. In Ref. [36], the authors also used the equilibrium QMC technique to extract the critical point $q_c = 0.21(4)$. In addition, our estimation of q_c has approximately the same error level as the equilibrium QMC result in Ref. [36]. However, since the accessible system size (up to $L = 256$) is much smaller than our result, it is possible that the equilibrium QMC study did not reach the region where the size effect in $q_c(L)$ becomes clear. Even though our result

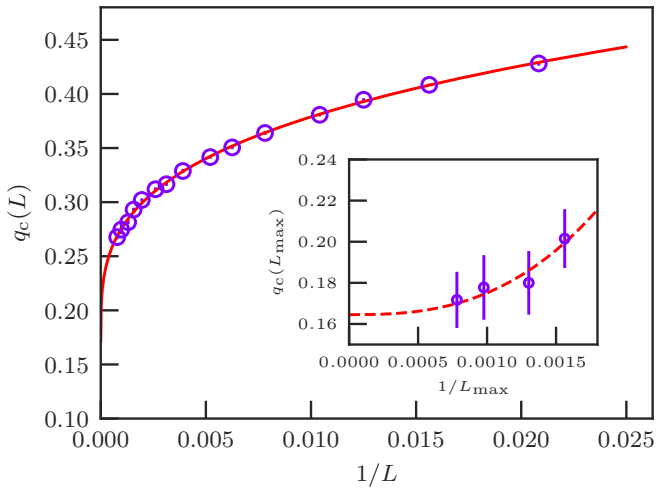

FIG. 2. Dependence on system size of the crossing point of $I(\tau)$ for L and $2L$. The solid line is a fit with the form of $q_c(L) = q_c + aL^{-\omega}$ to extract q_c in the thermodynamic limit. q_c is given by 0.170(14), with $a = 0.81(3)$, $\omega = 0.29(3)$, and χ^2 per degree of freedom of 1.04. Inset: Dependence of q_c on the largest system size L_{max} included in the fitting. The dashed line is a guide to the eyes.

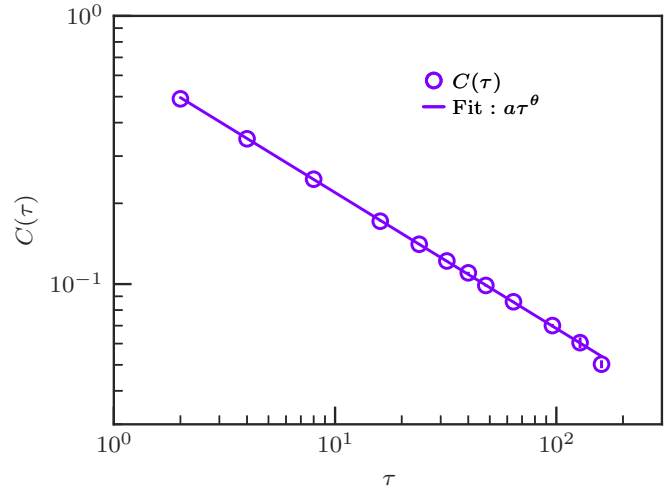

FIG. 3. Dependence of $C(\tau)$ on the evolution imaginary time τ with fixed $\tau L^{-z} = 1/16$. Power-law fitting shows the critical initial slip exponent $\theta = -0.507(3)$ with a prefactor $a = 0.704(6)$. Double logarithmic scales are used.

for q_c comes with a large error bar, the nonconverging convex behavior of $q_c(L)$ and slow decay of $I(\tau)$ on the QLRO side help to explain why it is difficult for QMC studies (either equilibrium or nonequilibrium) to extract the precise critical point. Certainly, our result can be improved by accessing larger system sizes and data of better quality, which will consume much more computational resources, and we will leave that to further studies. Since our estimation of $q_c = 0.170(14)$ has only moderate precision, we will use the ED estimation $q_c = 0.16478$ [36] in the following.

In Fig. 2, the aspect ratio τL^{-z} is fixed at $1/16$, but we have also tried different values of the aspect ratio (data not shown). For larger τL^{-z}, the curve of $q_c(L)$ moves downwards but also becomes flatter compared to the one shown here, which makes it more difficult to analyze the size effect. In addition, as τL^{-z} increases towards 1, the behavior of $q_c(L)$ converges to ground-state results, requiring many more computational resources. However, this does not mean that the smaller τL^{-z} is, the better. For small values, for instance, $\tau L^{-z} = 1/100$, the size required to reach the same scale of τ can be too large to simulate since τ should also exceed the microscopic time τ_{mic} so as not to fall in the nonuniversal stage. Therefore, it is better to choose a medium τL^{-z} based on the consideration of balancing the shape of $q_c(L)$, the system size available, and simulation time. Even so, the SITQCD can still save a large amount of computation efforts.

B. Determination of the exponent θ

In order to determine θ, we compute the imaginary-time correlation $C(\tau)$ for different L ranging from 32 to 2560 with $D_0 = 0$ according to Eq. (2.7). The aspect ratio is fixed at $\tau L^{-z} = 1/16$. As shown in Fig. 3, $C(\tau)$ does not increase with τ in the J-Q_3 spin chain, in contrast to the case of the quantum Ising model [14,21]. Instead, it decays with τ as a power law $C(\tau) \sim \tau^\theta$ with

$$\theta = -0.507(3).$$

To double-check the exponent θ given by $C(\tau)$, we study the behavior of $D(\tau)$ when the initial state has nonzero, but very, small D_0, which is close to its apparent zero fixed point. For a system of length L, the smallest positive value of D is $1/L$ (z component). This value is chosen as the initial D_0 for each size, and the evolution of D is shown in Fig. 4. In Fig. 4(a), it is clear that at the short-time stage, all $D(\tau)$ for various sizes satisfy a power law and the power-law range extends as L increases. From Eq. (2.3), one finds that $D(\tau) \simeq D_0\tau^\theta f(0,0) + O(L^{-1}\tau^{1/z})$. Thus, θ can be fitted by the short-time data of $D(\tau)$. We obtain θ as $\theta = -0.518(1)$ from the fitting of the data for $L = 1000$. This value is close to the one obtained from $C(\tau)$, as we discussed above. The deviation between the two estimations may be due to the finite length of the $L = 1000$ system, which is not large enough for $D(\tau)$ to get rid of the finite-size effect as for systems of different sizes, θ drifts slightly.

Additionally, in Fig. 4(a), one finds that $D(\tau)$ drops in later times towards zero. The dropping time is earlier for a system with a smaller size. This demonstrates that the finite-size effects control the scaling in the late-time stage. Also, it means that the higher-order terms of $L^{-1}\tau^{1/z}$ in the expansion of Eq. (2.3) dominate for large τ and small L. Moreover, for $g = 0$, Eq. (2.3) is equivalent to

$$D(\tau, g, D_0, L) = D_0 L^{\theta z} f_{DL}(L^{-z}\tau) \tag{4.1}$$

by the variable replacement. After rescaling $D(\tau)$ for different sizes according to Eq. (4.1) with $\theta = -0.507$ as input, we find in Fig. 4(b) that all curves collapse onto each other. This result not only confirms the value of θ but also verifies Eq. (4.1). Moreover, from Fig. 4(b), one finds that in the short-time region with small τ, $f_{DL}(L^{-z}\tau)$ satisfies $f_{DL}(L^{-z}\tau) \propto (L^{-z}\tau)^\theta$, which recovers Eq. (4.1) to $D(\tau) \propto D_0\tau^\theta$.

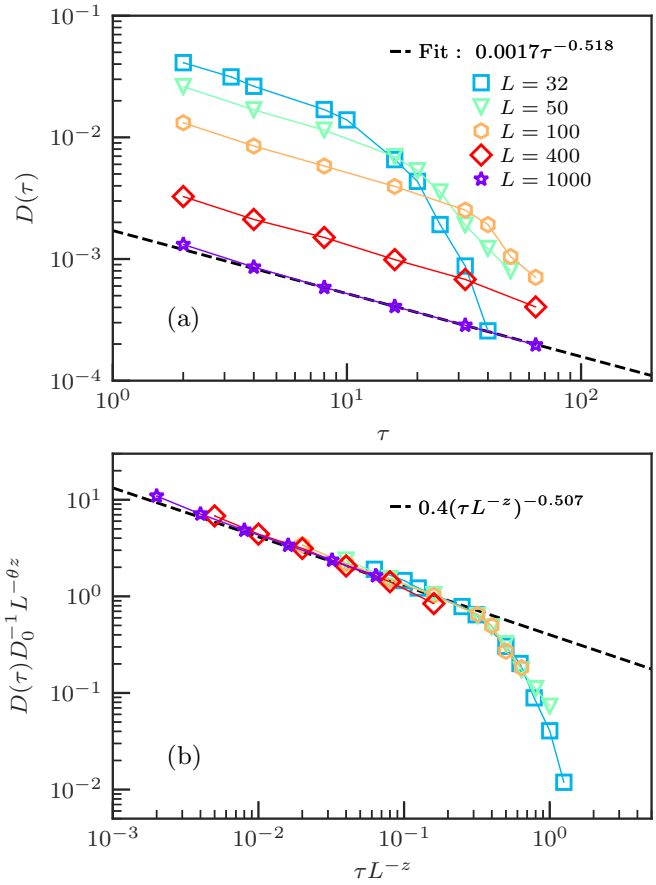

FIG. 4. (a) Dependence of $D(\tau)$ on the evolution imaginary time τ for various sizes as marked. (b) Rescaled curves for (a) according to Eq. (4.1). The dashed line in (a) is a power-law fit to show the exponent of $L = 1000$, while the one in (b) is plotted to show the power-law behaviors of the rescaled curves.

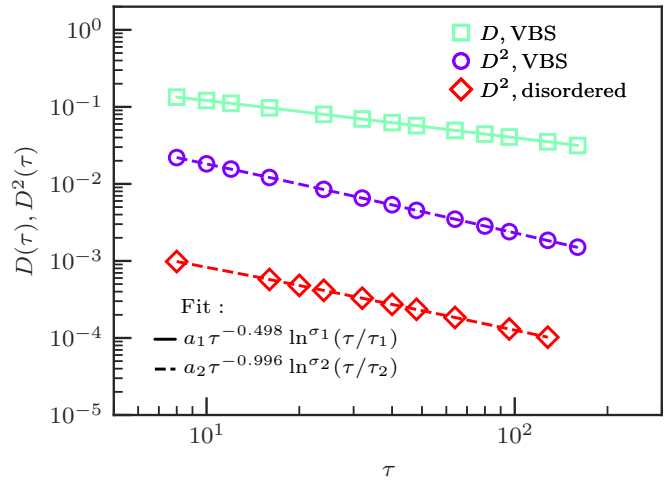

FIG. 5. Power-law decay of $D(\tau)$ and $D^2(\tau)$ for different initial conditions, with power corresponding to β/ν and $2\beta/\nu$, respectively. Multiplicative logarithmic corrections to the power laws are included in order to obtain good fits. The finial estimation of β/ν is given by 0.498(2).

C. Determination of the static exponent β/ν

Next, let us consider the static critical exponent β/ν. As pointed out already, $D_0 = D_{\rm sat}$ and $D_0 = 0$ are both apparent fixed points of Eq. (2.1), giving the scaling form of Eq. (2.5). Thus, we can estimate β/ν from these two different initial states here.

First, we consider $D_0 = D_{\rm sat}$. Here, the calculations are performed in the valence bond basis with $D_{\rm sat} = 3/8$. It is obvious that $D(\tau)$ and $D(\tau)^2$ should scale as $\tau^{-\beta/\nu z}$ and $\tau^{-2\beta/\nu z}$, respectively, for $g = 0$ and a fixed τL^{-z}. At longer times, $D(\tau)$ can be described using a power law. For $\tau = 32 - 160$, the fitting gives $\beta/\nu = 0.4919(2)$ along with a prefactor $a = 0.383(1)$. For τ ranging from 96 to 160, we find

$$\beta/\nu = 0.498(2),$$

with $a = 0.394(3)$. To be on the safe side, the value of 0.498(2) is used as our final estimation of β/ν. We will use this value to represent the asymptotic value of β/ν.

In order to include data from earlier times, by fixing $\beta/\nu = 0.498$, we consider a logarithmic correction in the fitting as

$$D(\tau) = a_1\tau^{-\beta/\nu}\ln^{\sigma_1}(\tau/\tau_1). \tag{4.2}$$

As shown in Fig. 5, we find that all data are well accounted for with the logarithmic correction. The fitting parameters are given by $a_1 = 0.3862(5)$, $\sigma_1 = 0.021(1)$, and $\tau_1 = 5.7(3)$. The logarithmic correction is actually not weak in this case.

Moreover, we observe a similar behavior in $D^2(\tau)$ with $D_0 = D_{\rm sat}$. With β/ν fixed at 0.498, we use the form of $D^2(\tau) = a_2\tau^{-2\beta/\nu}\ln^{\sigma_2}(\tau/\tau_2)$ to perform the fitting. We find that the curve is also well described, but the logarithmic correction appears to be stronger in $D^2(\tau)$ with $a_2 = 0.136(4)$, $\sigma_2 = 0.34(2)$, and $\tau_2 = 1.0(1)$.

To further confirm the value of β/ν, we consider the evolution starting from a disordered initial state with $D_0 = 0$. In this case $D(\tau)$ remains zero, and we study the behavior of $D^2(\tau)$. As seen in Fig. 5, the curve of $D^2(\tau)$ with $D_0 = 0$ is almost parallel to the corresponding curve with $D_0 = D_{\rm sat}$, indicating identical critical exponents. By setting $\beta/\nu = 0.498$ as the input, we perform the fitting using the same functional form and find $a_2 = 0.0025(2)$, $\sigma_2 = 0.88(2)$, and $\tau_2 = 0.21(3)$ for $D^2(\tau)$ with $D_0 = 0$. The deviation between $D^2(\tau)$ in Fig. 5 comes from the different definitions of the order parameter (full component for $D_{\rm sat}$ and the z component for the disordered case). In all cases, when including the logarithmic term and allowing the power β/ν to vary, the fittings give β/ν equal to 0.511(6), 0.48(1), and 0.53(3) for $D(\tau)$, $D^2(\tau)$ with $D_0 = D_{\rm sat}$, and $D^2(\tau)$ with $D_0 = 0$, respectively. These results are in agreement with 0.498(2) extracted from the behavior of $D(\tau)$ at longer times.

Even though the origin of the logarithmic corrections is not totally clear to us, we hereby discuss the possible reasons of their presence. In the fittings, these corrections are introduced in order to include the data at earlier times with β/ν fixed at the result extracted from the longer times, i.e., $\beta/\nu = 0.498$. However, in the short-imaginary-time scaling forms of $D(\tau)$ and $D^2(\tau)$, we did not consider the short-time corrections independently, like the finite-size corrections considered in equilibrium studies. Therefore, it is possible that the short-time scaling corrections are responsible for the

presence of the logarithmic corrections. Another possibility is the inaccurate estimate of the critical point. In the field-theory description, the QLRO-VBS transition is driven by a marginal irrelevant operator. This marginal operator causes multiplicative logarithmic corrections in the QLRO phase, but exactly at the critical point, the logarithmic correction should vanish [37,38]. However, as pointed out already, it is difficult to extract the exact critical point in our study. It is also possible $q_c = 0.16478$, which we took from the ED study [36], does not catch the exact critical point, thus causing the logarithmic corrections.

As mentioned above, the same kind of dimerization transition in this model also occurs in the frustrated J_1-J_2 spin chain. A recent work [39] on the $S = 1/2$ J_1-J_2 XYZ chain pointed out that for the isotropic J_1-J_2 spin chain, the dynamical exponent $z = 1$ and the critical exponent η should equal to 1, which indicates that β/ν is 1/2, agreeing with our estimation of $\beta/\nu = 0.498(2)$. This consistency between our result and theirs not only confirms that the J-Q_3 spin chain (1.1) belongs to the same universality class with the J_1-J_2 spin chain, as pointed out previously [24,25,36,40,41], but also shows again the validity of the SITQCD method. In addition, the QLRO-VBS transition in the J_1-J_2 chain is closely related to the spontaneous dimerization occurring in the spin-Peierls compound $CuGeO_3$ [42,43]. Our results for the J-Q_3 chain provide alternative access to the same physics and inspire further experimental and computational explorations of the nature of the dimerization transition [24,25,36,40,41].

D. D_0 as a marginal scaling variable

By comparing the value of θ and β/ν, we can find that their absolute values are very close to each other. According to Eq. (2.4), we infer that the initial order parameter D_0 is a marginal scaling variable with $x_0 = 0$. Under scale transformation in Eq. (2.1), D_0 does not change. Accordingly, besides the two apparent fixed points, i.e., $D_0 = 0$ and $D_0 = D_{\rm sat}$, all D_0 with zero initial correlation are fixed points of the transformation. As a result, Eq. (2.5) should be applicable for all D_0 but with different scaling functions $f_{D^k,D_0}(gL^{\frac{1}{\nu}}, \tau L^{-z})$.

Here, we argue that $f_{D^1,D_0}(0,x) = D_0 f_{D^1}(0,x)$ for any D_0. This equation is a direct generalization of Eq. (2.3). Note that in Eq. (2.3), a small D_0 is required. Since $\theta = -\beta/\nu z$ with $z = 1$, Eq. (2.3) becomes $D(\tau) = D_0 \tau^{-\beta/\nu z} f_D(0,x)$ for small D_0. This scaling function is then identical to Eq. (2.5), which is valid for $D_0 = D_{\rm sat}$ since $D(\tau = 0) = D_0$. Namely, the relation $f_{D^1,D_0}(0,x) = D_0 f_{D^1}(0,x)$ is valid not only for small D_0 but also for the maximum $D_{\rm sat}$. In addition, in the short-time region, the scaling function is continuous in terms of D_0. Therefore, one can conjecture that this relation should be valid for any value of D_0, such that the evolution of $D(\tau)$ satisfies

$$D(\tau, L^{-1}) = D_0 \tau^{-\frac{\beta}{\nu z}} f(g\tau^{\frac{1}{\nu z}}, L^{-1}\tau^{\frac{1}{z}}), \tag{4.3}$$

in which the scaling function f does not depend on D_0.

To examine Eq. (4.3), we consider the imaginary-time relaxation of $D(\tau)$ for various system sizes at $g = 0$. In Fig. 6(a), we find that $D(\tau)$ increases as D_0 increases. Moreover, for all D_0, in the short-time stage, $D(\tau) \propto \tau^{\theta} \sim \tau^{-\beta/\nu z}$. This indicates that for the purpose of extracting θ or β/ν, D_0 is not necessarily restricted to small values in this situation. In the late-time stage, the information contained in initial D_0 is "forgotten," and the curves for various D_0 tend to merge. In Fig. 6(b), we rescale $D(\tau)$ with D_0 and find that all curves match each other according to Eq. (4.3), showing that the scaling function f does not depend on D_0 indeed.

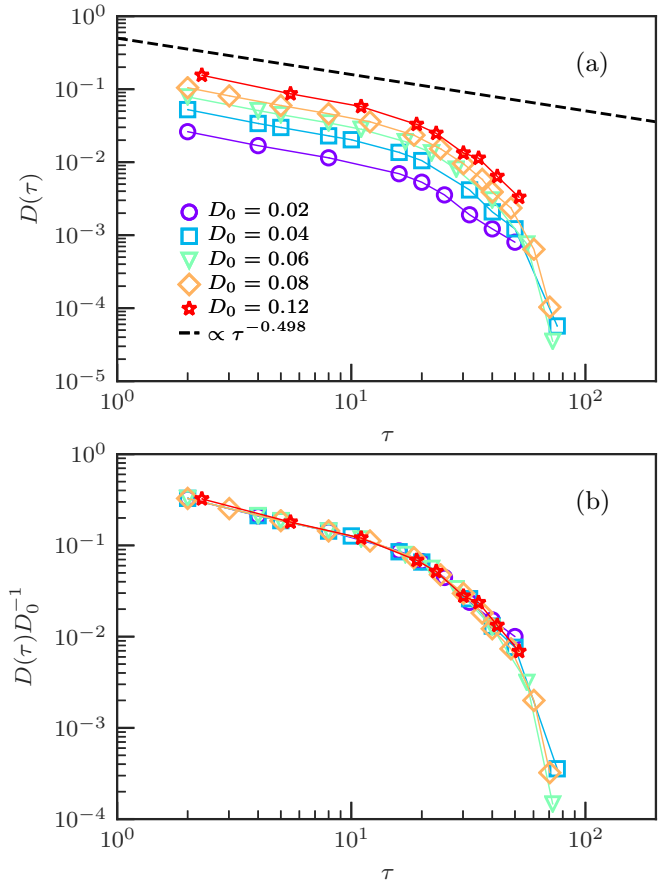

FIG. 6. For a system with fixed $L = 50$, curves of $D(\tau)$ versus τ (a) before and (b) after rescaling according to Eq. (4.3). For different D_0, $D(\tau)$ decays with almost the same exponent at earlier times, as indicated by the dashed line in (a).

Based on this, it is tempting to examine the behavior of $D(\tau)$ when the initial state has magnetic order. We can infer that even if the system is relaxed from an AF state with $D_0 = 0$, Eq. (4.3) should still be satisfied as long as the correlation length vanishes. In Fig. 7, we show the behavior of $D^2(\tau)$ instead of $D(\tau)$ as $D(\tau)$ is zero in this case. It is obvious that at the critical point, $D^2(\tau) \sim \tau^{-0.996}$, multiplied by a logarithmic correction with $a = 0.10(4)$, $\tau_0 = 0.04(3)$, and $\sigma = 1.2(2)$. The behavior of $D^2(\tau)$ is very similar to the results with $D_0 = D_{\rm sat}$ or $D_0 = 0$ shown in Fig. 5. Such a result again reflects the marginal role of D_0 in the imaginary-time relaxation process.

V. DISCUSSION

Here, we discuss the possible reasons for the marginal D_0. In the quantum Ising model, the positive θ is induced by the fact that the critical point is shifted down towards the ordered phase compared with its mean-field value. Thus, the uncorrelated initial state "feels" an ordered phase when the system is

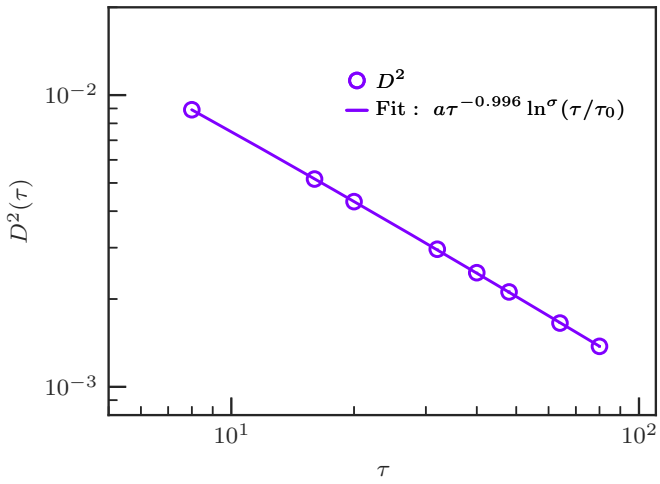

FIG. 7. Dependence of D^2 on τ at the critical point relaxed from an AF starting state with $\tau L^{-z} = 1/16$. $D^2(\tau)$ obeys Eq. (4.3) as well.

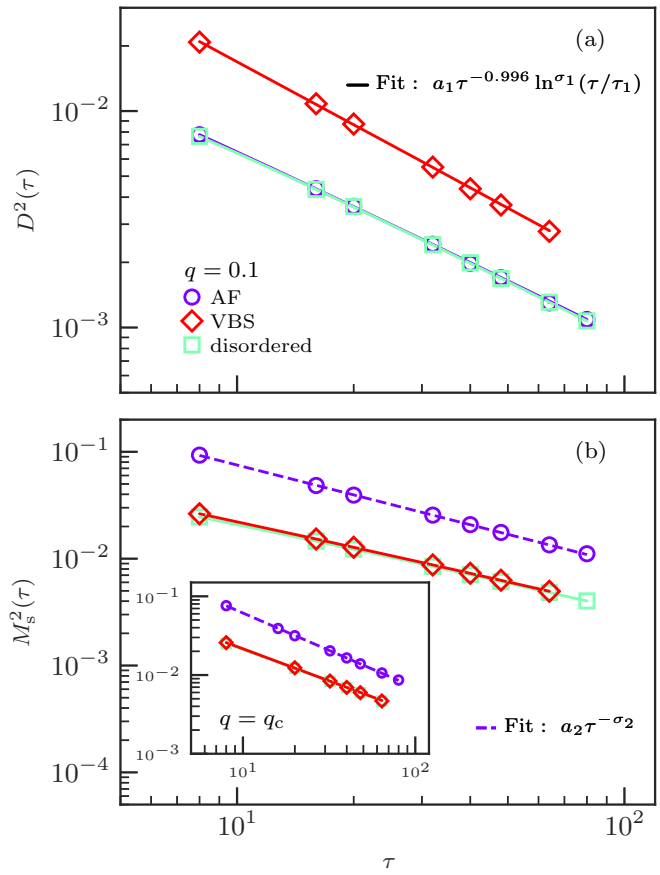

FIG. 8. Dependence of M_s^2 and D^2 on τ when relaxed from the AF/VBS/disordered state to $q = 0.1$ and $q = q_c$ with $\tau L^{-z} = 1/16$. The solid and dashed lines correspond to a power-law form with and without logarithmic correction, respectively. The behaviors of $M_s^2(\tau)$ and $D^2(\tau)$ are discussed in the text.

in the vicinity of the real critical point [14]. In contrast, in the present case, the QLRO phase is a critical phase. Therefore, there is no proper mean-field solution for this model. In addition, the gap in the VBS phase is induced by a marginally relevant operator in the VBS phase from the field theory, and this leads to the opening of an initially exponentially small gap [37,38], in contrast to the Ising case in which the gap is a power function of the distance to the critical point. These elements make the phase transition seem quite soft compared with the Ising case. The initial order parameter thus plays only a marginal role in the imaginary-time relaxation process.

Since the perturbation which drives the dimerization transition in the J-Q_3 model is marginally irrelevant in the QLRO phase, we can infer that the scaling properties discussed above are also applicable in the QLRO phase up to a logarithmic correction [37,38]. To examine this, we perform QMC simulations with various initial states in the QLRO gapless phase. We find that for fixed $\tau L^{-z} = 1/16$, $D^2(\tau)$ satisfies $D^2(\tau) \sim \tau^{-0.996}$ with a logarithmic correction, as shown in Fig. 8(a). The fitting parameters are given by $a_1 = 0.1717(5)$, $\tau_1 = 6.8(6)$, $\sigma_1 = 0.021(5)$ for the VBS initial state; $a_1 = 0.044(3)$, $\tau_1 = 1.0(2)$, $\sigma_1 = 0.44(3)$ for the disordered initial state; and $a_1 = 0.021(6)$, $\tau_1 = 0.12(9)$, $\sigma_1 = 0.7(1)$ for the AF initial state. The exponent therein is quite close to $2\beta/\nu z$ as at the critical point.

In addition, in Fig. 8(b), we also show the scaling behavior of the magnetic order parameter, which is defined as $\mathbf{M}_s = [\sum_i^L (-1)^i \mathbf{S}_i]/L$. We find that the squared staggered magnetization $M_s^2(\tau)$ also obeys the scaling behavior $M_s^2(\tau) \sim \tau^{-0.996}$ multiplied by a logarithmic correction term for the VBS and disordered initial state. For the VBS case, we have $a_1 = 0.026(1)$, $\tau_1 = 0.04(3)$, and $\sigma_1 = 1.2(2)$. For the disordered case, $a_1 = 0.024(7)$, $\tau_1 = 0.05(2)$, and $\sigma_1 = 1.3(1)$. When the initial state has AF order, the logarithmic correction appears to be very weak, and we instead use the pure power-law form in the fitting. We find the power is $\sigma_2 = 0.920(2)$ with $a_2 = 0.620(4)$, slightly different from the other two cases. This may because the AF state is very far from the QLRO phase and the evolution time $\tau = L^z/16$ is so short. Whether there is a logarithmic correction in this situation needs more careful analysis. In the inset of Fig. 8(b), we show $M_s^2(\tau)$ at the critical point. We find that they obey the same scaling behavior as in the QLRO phase. Here, we list the fitting parameter at $g = 0$ for further reference. For the VBS case, $a_1 = 0.05(1)$, $\tau_1 = 0.11(6)$, and $\sigma_1 = 0.94(9)$. For the disordered case, $a_1 = 0.072(2)$, $\tau_1 = 0.3(1)$, and $\sigma_1 = 0.82(9)$. For the AF case, we use the pure power-law form, which gives $\sigma_2 = 0.938(1)$ and $a_2 = 0.525(2)$. As discussed above, the logarithmic corrections found here could be induced by short-time scaling corrections or an inaccurate value of the critical point. Finding the origin of the logarithmic corrections is beyond the purpose of this study, and we will leave it to future studies.

VI. SUMMARY

In this work, we studied the SITQCD of the QLRO-VBS transition in the J-Q_3 chain. Using the method based on the scaling theory of the SITQCD, we determined its critical point to be $q_c = 0.170(14)$, in agreement with a recent ED and QMC study [36]. Then we determined the critical initial slip exponent $\theta = -0.507(3)$ and the static exponent $\beta/\nu = 0.498(2)$. Moreover, by comparing the value of θ and

β/ν, we found that the initial order parameter D_0 is a marginal scaling variable. This is quite different from the case in the quantum Ising model, in which the initial order parameter is a relevant scaling variable [14,21]. We showed that the marginal D_0 leads to a short-time decay of the order parameter, rather than the initial increase as shown in the quantum Ising model [14,21]. We also argued that the reason for the appearance of the marginal initial order parameter is that this phase transition is induced by a perturbation which is marginally irrelevant in the QLRO phase and marginally relevant in the VBS phase [37,38]. Accordingly, we also showed that the scaling theory of the SITQCD at the critical point is also applicable in the QLRO phase only up to a logarithmic scaling correction.

Recently, the critical initial slip behavior was also found theoretically in the prethermal real-time dynamics [44–53]. In particular, a negative initial slip exponent was also found in the quench dynamics of the Dirac systems [54]. Accordingly, it is instructive to study the real-time relaxation dynamics of J-Q_3 model, which we leave as future work. In addition, due to the similarity between the imaginary-time relaxation and boundary effect in real space, it is also interesting to consider the effect of a marginal D_0 in real space [55]. In a system with the boundary set to have a fixed local D_0, the dependence of D on the distance to the boundary r should obey $D(r) \sim r^{-\beta/\nu}$ if D_0 is marginal. The effect of D_0 is not propagated through space due to its marginal role. This issue is also worth investigating. More interestingly, the two-dimensional J-Q_3 model hosts a Néel-VBS quantum phase transition beyond the Landau-Ginzburg-Wilson (LGW) paradigm [23,56]. The SITQCD has proved applicable in LGW phase transitions as well as topological quantum phase transitions [14]. The SITQCD in the deconfined quantum phase transition framework is very intriguing, and that work is in process.

ACKNOWLEDGMENTS

The authors are grateful to A. W. Sandvik for his valuable discussions. Y.-R.S. acknowledges support from Grant No. NSFC-11947035 and the startup grant (Grant No. RP2020120) at Guangzhou University. S.Y. is supported by the startup grant (Grant No. 74130-18841229) at Sun Yat-Sen University.

[1] J. Dziarmaga, Adv. Phys. **59**, 1063 (2010).
[2] A. Polkovnikov, K. Sengupta, A. Silva, and M. Vengalattore, Rev. Mod. Phys. **83**, 863 (2011).
[3] P. J. Love, Nat. Phys. **16**, 130 (2020).
[4] M. Motta, C. Sun, A. T. K. Tan, M. J. O'Rourke, E. Ye, A. J. Minnich, F. G. S. L. Brandão, and G. K.-L. Chan, Nat. Phys. **16**, 205 (2020).
[5] C. De Grandi, A. Polkovnikov, and A. W. Sandvik, Phys. Rev. B **84**, 224303 (2011).
[6] C. D. Grandi, A. Polkovnikov, and A. W. Sandvik, J. Phys.: Condens. Matter **25**, 404216 (2013).
[7] C.-W. Liu, A. Polkovnikov, and A. W. Sandvik, Phys. Rev. B **87**, 174302 (2013).
[8] A. Avdoshkin and A. Dymarsky, arXiv:1911.09672.
[9] M. J. S. Beach, R. G. Melko, T. Grover, and T. H. Hsieh, Phys. Rev. B **100**, 094434 (2019).
[10] A. W. Sandvik, *Lectures on the Physics of Strongly Correlated Systems XIV: Fourteenth Training Course in the Physics of Strongly Correlated Systems*, AIP Conf. Proc. No. **1297**, 135 (2010).
[11] H. K. Janssen, B. Schaub, and B. Schmittmann, Z. Phys. B **73**, 539 (1989).
[12] D. A. Huse, Phys. Rev. B **40**, 304 (1989).
[13] E. V. Albano, M. A. Bab, G. Baglietto, R. A. Borzi, T. S. Grigera, E. S. Loscar, D. E. Rodriguez, M. L. R. Puzzo, and G. P. Saracco, Rep. Prog. Phys. **74**, 026501 (2011).
[14] S. Yin, P. Mai, and F. Zhong, Phys. Rev. B **89**, 144115 (2014).
[15] S. Zhang, S. Yin, and F. Zhong, Phys. Rev. E **90**, 042104 (2014).
[16] Z. B. Li, U. Ritschel, and B. Zheng, J. Phys. A **27**, L837 (1994).
[17] Z. B. Li, L. Schülke, and B. Zheng, Phys. Rev. Lett. **74**, 3396 (1995).
[18] Z. Li, L. Schülke, and B. Zheng, Phys. Rev. E **53**, 2940 (1996).
[19] B. Zheng, Phys. Rev. Lett. **77**, 679 (1996).
[20] B. Zheng, Int. J. Mod. Phys. B **12**, 1419 (1998).
[21] Y.-R. Shu, S. Yin, and D.-X. Yao, Phys. Rev. B **96**, 094304 (2017).
[22] S. Sachdev, *Quantum Phase Transitions* (Cambridge University Press, Cambridge, 1999).
[23] A. W. Sandvik, Phys. Rev. Lett. **98**, 227202 (2007).
[24] Y. Tang and A. W. Sandvik, Phys. Rev. Lett. **107**, 157201 (2011).
[25] S. Sanyal, A. Banerjee, and K. Damle, Phys. Rev. B **84**, 235129 (2011).
[26] K. Okamoto and K. Nomura, Phys. Lett. A **169**, 433 (1992).
[27] S. Eggert, Phys. Rev. B **54**, R9612 (1996).
[28] J. Zinn-Justin, *Quantum Field Theory and Critical Phenomena* (Clarendon, Oxford, 1996).
[29] A. Altland and B. Simons, *Condensed Matter Field Theory* (Cambridge University Press, Cambridge, 2006).
[30] T. Tomé and M. J. de Oliveira, Phys. Rev. E **58**, 4242 (1998).
[31] P. M. C. de Oliveira, Europhys. Lett. **20**, 621 (1992).
[32] M. Silvério Soares, J. Kamphorst Leal da Silva, and F. C. SáBarreto, Phys. Rev. B **55**, 1021 (1997).
[33] E. Farhi, D. Gosset, I. Hen, A. W. Sandvik, P. Shor, A. P. Young, and F. Zamponi, Phys. Rev. A **86**, 052334 (2012).
[34] K. Beach and A. W. Sandvik, Nucl. Phys. B **750**, 142 (2006).
[35] K. Binder, Phys. Rev. Lett. **47**, 693 (1981).
[36] S. Yang, D.-X. Yao, and A. W. Sandvik, arXiv:2001.02821.
[37] I. Affleck, Phys. Rev. Lett. **55**, 1355 (1985).
[38] I. Affleck and F. D. M. Haldane, Phys. Rev. B **36**, 5291 (1987).
[39] C. Mudry, A. Furusaki, T. Morimoto, and T. Hikihara, Phys. Rev. B **99**, 205153 (2019).
[40] Y. Tang and A. W. Sandvik, Phys. Rev. B **92**, 184425 (2015).
[41] P. Patil, E. Katz, and A. W. Sandvik, Phys. Rev. B **98**, 014414 (2018).
[42] G. S. Uhrig, Phys. Rev. B **57**, R14004 (1998).

[43] A. Weiße, G. Wellein, and H. Fehske, Phys. Rev. B **60**, 6566 (1999).
[44] P. Gagel, P. P. Orth, and J. Schmalian, Phys. Rev. Lett. **113**, 220401 (2014).
[45] P. Gagel, P. P. Orth, and J. Schmalian, Phys. Rev. B **92**, 115121 (2015).
[46] P. Calabrese, F. H. L. Essler, and M. Fagotti, J. Stat. Mech. (2012) P07016.
[47] P. Calabrese, F. H. L. Essler, and M. Fagotti, J. Stat. Mech. (2012) P07022.
[48] A. Maraga, A. Chiocchetta, A. Mitra, and A. Gambassi, Phys. Rev. E **92**, 042151 (2015).
[49] A. Chiocchetta, M. Tavora, A. Gambassi, and A. Mitra, Phys. Rev. B **91**, 220302(R) (2015).
[50] A. Chiocchetta, M. Tavora, A. Gambassi, and A. Mitra, Phys. Rev. B **94**, 134311 (2016).
[51] A. Chiocchetta, A. Gambassi, S. Diehl, and J. Marino, Phys. Rev. B **94**, 174301 (2016).
[52] A. Chiocchetta, A. Gambassi, S. Diehl, and J. Marino, Phys. Rev. Lett. **118**, 135701 (2017).
[53] W. Liu and U. C. Täuber, J. Phys. A. **49**, 434001 (2016).
[54] S.-K. Jian, S. Yin, and B. Swingle, Phys. Rev. Lett. **123**, 170606 (2019).
[55] H.-W. Diehl, in *Phase Transitions and Critical Phenomena*, edited by C. Domb and J. L. Lobowitz (Academic, London, 1986), p. 75.
[56] T. Senthil, A. Vishwanath, L. Balents, S. Sachdev, and M. P. A. Fisher, Science **303**, 1490 (2004).